Atmos. Chem. Phys. Discuss., 12, 31871–31916, 2012
www.atmos-chem-phys-discuss.net/12/31871/2012/
doi:10.5194/acpd-12-31871-2012

Atmospheric Chemistry and Physics Discussions

Wintertime peroxyacetyl nitrate (PAN) in the megacity Beijing: the role of photochemical and meteorological processes

H. Zhang[1], X. Xu[1], W. Lin[1,2], and Y. Wang[1]

[1]CMA Key Laboratory for Atmospheric Chemistry, Institute of Atmospheric Composition, Chinese Academy of Meteorological Sciences, Beijing, 100081, China
[2]CMA Meteorological Observation Centre, Beijing, 100081, China

Received: 4 November 2012 – Accepted: 3 December 2012 – Published: 11 December 2012

Correspondence to: X. Xu (xuxb@cams.cma.gov.cn)

Published by Copernicus Publications on behalf of the European Geosciences Union.

Abstract

Peroxyacetyl nitrate (PAN) is one of the key photochemical pollutants and acts as an important reservoir for the peroxyacetyl (PA) radical and nitrogen oxides (NO_x) over cold and less polluted regions. Previous measurements of PAN in Asian megacities were scarce and mainly conducted for relatively short periods in summer. In this study, we present and analyze the measurements of PAN, O_3, NO_x, CO, and some meteorological variables, made at an urban site (CMA) in Beijing from 25 January to 22 March 2010. During the observations, the hourly concentration of PAN varied from 0.23 to 3.51 ppb, with an average of 0.70 ppb. Both PAN and O_3 showed small but significant diurnal cycle, with PAN peaking around 17:00 LT, three hours later than O_3. The observed concentration of PAN is well correlated with that of NO_x but not O_3. These phenomena indicate that the variations of the winter concentrations of PAN and O_3 in urban Beijing are decoupled with each other. Wind conditions and transport of air masses exert very significant impacts on O_3, PAN, and other species. The strong WNW-N winds caused elevated concentrations of surface O_3 and lower concentrations of PAN, NO_x, and CO. Weak winds from the other directions led to enhanced levels of PAN, NO_x, and CO and decreased level of O_3. Air masses arriving at our site originated either from the boundary layer over the highly polluted N-S-W sector or from the free troposphere over the W-N sector. The descending free-tropospheric air was rich in O_3, with an average PAN/O_3 ratio smaller than 0.031, while the boundary layer air over the polluted sector contained higher levels of PAN and primary pollutants, with an average PAN/O_3 ratio of 0.11. These facts related with meteorological conditions, specifically the air transport conditions, can well explain the observed PAN-O_3 decoupling. The impact of meso-scale transport is demonstrated using a case during 21–22 February 2010. In addition to transport, photochemical production is important to PAN in the winter boundary layer over Beijing. The PA concentration is estimated from the measurements of PAN and related variables. The estimated PA concentration for three days with stable atmospheric condition, 7 February, 23 February, and 11 March, are in the

range of 0–0.012, 0–0.036, and 0–0.040 ppt, respectively. We found that both the formation reaction and thermal decomposition contributed significantly to PAN's variation. The results here suggest that even in the colder period, both photochemical production and thermal decomposition of PAN in the polluted boundary layer over Beijing are not negligible, with the production exceeding the decomposition.

1 Introduction

Peroxyacetyl nitrate (PAN, $CH_3COO_2NO_2$) in the atmosphere is exclusively produced by photochemical reactions and plays an important role in local, regional and global atmospheric chemistry (Kourtidis et al., 1993; Nielsen et al., 1981; Williams et al., 1993). Studies suggest that PAN is one of the important indicator compounds of peroxy radical activity in an urban airshed (Finlayson-Pitts and Pitts, 2000; Gaffney et al., 1989) and photochemical smog episodes (Bottenheim et al., 1994; Rappenglück et al., 2003). In addition, PAN is toxic to human health and harmful to vegetation growth as well (Kleindienst et al., 1990; Peak and Belser, 1969; Stephens, 1969; Taylor, 1969). Since its discovery in Los Angeles air by Stephens et al. (1956), PAN has been observed in many field campaigns in different regions and found to be globally ubiquitous (Singh and Salas, 1983b, 1989). The reported PAN level ranges from a few ppt in marine background air to higher than 30 ppb in urban air (e.g. Grosjean, 1988, 2003; Marley et al., 2007; Roberts et al., 2002, 2007; Schmitt and Volz-Thomas, 1997; Singh and Salas, 1989; Whalley et al., 2004; Williams et al., 1993, 1997).

Both PAN and O_3 are important oxidants and secondary pollutants in the atmosphere. They have common chemical sources, i.e. the photochemical reactions among NO_x, VOCs, etc. While O_3 in the troposphere can be produced from precursors other than VOCs, e.g. CO, CH_4 (Chameides and Walker, 1973) or originates from the stratosphere (Staehelin et al., 2001), PAN is only produced from those VOCs that can form the acetyl radical CH_3CO or peroxyacetyl (PA) radical CH_3COO_2 (Grosjean et al., 2002; LaFranchi et al., 2009; Liu et al., 2010). Reaction with OH radical and photolysis can

remove PAN from the atmosphere (Singh, 1987; Talukdar et al., 1995). For PAN in the boundary layer, however, the most effective sink is thermal decomposition (Cox and Roffey, 1977; Singh, 1987; Tuazon et al., 1991). In addition, the dry deposition of PAN over vegetation has been found to be significant (Schrimpf et al., 1996; Turnipseed et al., 2006; Wu et al., 2012). Thermal decomposition of PAN is highly dependent on temperature (Cox and Roffey, 1977; Tuazon et al., 1991). The lifetime of PAN is as short as 30 min at 300 K, but as long as a month at 260 K (Tang et al., 2001). Therefore, PAN can be transported over a long-range in cold environment, for instance, winter and upper troposphere (Corkum et al., 1986; Fischer et al., 2011; Rappenglück et al., 2003, 2004), causing the dispersion of PAN over remote ocean areas (Jacobi et al., 1999), the polar regions (Beine and Krognes, 2000; Bottenheim et al., 1986, 1993; Dassau et al., 2004; Jacobi et al., 2000), and even in the free troposphere (Fischer et al., 2011; Singh and Sales, 1983a). The ubiquitous existence and thermal instability make PAN a reservoir for NO_x and the PA radical, and hence PAN plays an important role in the production of O_3 in remote areas (Aneja et al., 1999; Crutzen, 1979; Derwent and Jenkin, 1991; Gaffney et al., 1993; Hudman et al., 2004; Ridley et al., 1990; Singh et al., 1992; Suppan et al., 1998).

Due to the ever increasing emissions of NO_x, VOCs, etc., photochemical pollution has become one of the air quality problems in Beijing and surrounding areas. High levels of surface O_3 are often observed in warmer months (Lin et al., 2008; Wang et al., 2006) and increase trends have been reported for O_3 in different layers of the troposphere (Ding et al., 2008; Tang et al., 2009; Wang et al., 2012), indicating the existence of photochemical smog in the region. While data of surface O_3 in the greater Beijing area are relatively plentiful, measurements of PAN are quite scarce. The first measurements of PAN at an urban site in Beijing showed a maximum concentration of 6.8 ppb in May 1990 (Zhang and Tang, 1994). Even higher peak levels were observed during summer in later studies (Zhang et al., 2011). All these previous measurements are either discontinuous or very short-term based (< two weeks). In addition, measurements of PAN in Beijing from other seasons are lacking. In this paper, we present

measurements of PAN, O_3, and some related species in the urban area of Beijing during a winter/spring period. We characterize the measurements and discuss the relationships among species and impacts of meteorological conditions on the measurements. In addition, we make an estimation of the concentration of the PA radical based on our observations.

2 Methods

2.1 Observations

From 25 January to 22 March 2010, the concentrations of PAN, O_3, and some related species were observed in the urban area of Beijing. The city Beijing is the capital of China and one of the megacities in the world. It is situated in a transition zone from mountainous region to the North China Plain (NCP), a region with two megacities Beijing and Tianjin (about 110 km from Beijing, Fig. 1) and many other cities and townships. This makes the air quality of Beijing subject to the influences from emissions in the NCP. Beijing City had a population of 20.186 millions by the end of 2011 (http://zhengwu.beijing.gov.cn/tjxx/tjgb/t1219544.htm). With strong increasing trends of residents and vehicles since about two decades, traffic related emissions have created challenges to the improving the urban air quality (Wu et al., 2011). In the cold months, heating related emissions can make substantial contributions to the levels of air pollutants (Lin et al., 2011).

The observations were made at an office building of Chinese Meteorological Administration (CMA, 39.95° N, 116.32° E, 58 m a.s.l.), located between the 2nd and 3rd ring roads of Beijing (see details in Lin et al., 2011). The PAN analyzer (Meteorologie Consult GmbH, Germany) that we used consists of an automated gas chromatograph (GC) equipped with an electron capture detector (ECD) and a calibration unit. A specific PC-software was used to collect and handle chromatographic data at a resolution of 10-min. The analyzer is virtually the same type as the one reported by Volz-Thomas

et al. (2002), but the separation is optimized only for PAN and CCl_4 and acetone instead of acetaldehyde is used to produce PAN standards. The analyzer was calibrated in variable intervals (respectively on 26 January, 27 January, 28 January, 29 January, 31 January, 1 February, 4 February, 10 February, 4 March, and 22 March, 2010) during the observation period and each calibration process lasted for 1–2 h. When calibrating, the PAN standard was prepared by introducing an NO standard in nitrogen (9.81 ppm, produced by Scottgas, USA) to react with acetone vapor under the irradiating of a UV lamp. For the ten calibrations, the analyzer sensitivity (peak area per ppb PAN) averaged 33 306, with a relative deviation of 7.5 %. There was no clear trend in the sensitivity. Therefore, all measurements of ambient PAN were calibrated using the average sensitivity for the whole observation period. The detection limit of the analyzer is about 50 ppt. More details about the PAN detecting system can be seen in literature (Volz-Thomas et al., 2002; Zellweger et al., 2000; Zhang et al., 2009).

O_3, NO/NO_2/NO_x, and CO were simultaneously observed using a set of commercial instruments, i.e. an O_3 analyzer (Model 49C), a NO_x analyzer (Model 42CTL) with a molybdenum NO_2-to-NO converter, and a CO analyzer (Model 48CTL), respectively, from Thermo Environmental Instruments, Inc., USA. Zero/span checks and multi-point calibrations were carried in the way described in Lin et al. (2011). All signals were acquired every second and averaged to obtain 1-min average data. All instruments were installed in an air-conditioned room. More details about the instrumentation are given in Lin et al. (2011).

2.2 Simulations

For the analysis and interpretation of the measurements, calculations of backward trajectories of air-masses were performed using the HYSPLIT4 trajectory model (Version 4.9), developed by the National Oceanic and Atmospheric Administration (NOAA) Air Resources Laboratory (Draxler and Hess, 1997). GDAS dataset (3 hourly, global, $1° \times 1°$ in longitude and latitude, and 23 pressure levels) was used for the meteorological input. 24-h backward trajectories were calculated for air parcels arriving

at 100 m above the ground level of the observation site. In addition, a meso-scale model (WRF Version 3; http://www.wrf-model.org/index.php; Skamarock et al., 2008) was used to simulate the meteorological fields in Beijing and the surrounding area. The simulations were nested for 3 domains, with the smallest one containing the NCP. The WRF Model was run every time for a 24-h period starting from 00:00 on the 21 February (Beijing local time). Schemes of microphysical processes, ground layer, boundary layer, and diffusion options are set as FERRIER (NEW ETA; Ferrier et al., 2002), MONIN-OBUKHOV (Monin and Obukhov, 1954), YSU (Hong and Dudhia, 2003), and OLD SCHEME (see http://www.mmm.ucar.edu/wrf/users/docs/user_guide/users_guide_chap5.html#Phys), respectively.

3 Results and discussion

3.1 Time series and characteristics

The time series of observed concentrations of PAN, O_3, NO, NO_2, and CO, together with those of temperature (T), wind vector, and global radiation (G), are plotted in Fig. 2. According to the observation results, PAN plumes are obvious as several pronounced peaks over 1 ppb were detected. There was also a slight increase trend in the baseline level of PAN as the season shifted from winter to early spring. The phenomenon here is inconsistent with some other experimental results demonstrating PAN's annual variation with elevated winter level and descending summer level because a greater net loss of PAN through thermal decomposition would appear in warmer situation (Beine and Krognes, 2000). The reason for this feature is partly because that as warmer season commences, solar radiation would enhance and promote more photochemical reactions, thus makes thermal decomposition incapable to offset increasing production rate. Apart from this reason, attention should also be paid to the variations of the precursor concentrations and other meteorological conditions. Figure 2 displays no affirmative trends in the concentrations of NO_x and CO. Therefore, it seems that the changes of

radiation and probably other meteorological conditions were more important factors for the observed PAN trend.

It is noticeable from Fig. 2 that the periods with higher PAN levels correspond to lower O_3 levels and higher levels of CO and NO_x, and those with lower PAN levels correspond usually to higher O_3 levels. This reveals a fact that the variations of the two photochemical oxidants, O_3 and PAN, were decoupled. Since the plumes with higher PAN levels lasted for several days, the decoupling was not caused by any differences in diurnal patterns of O_3 and PAN. Further discussions about this are given in latter sections.

3.2 Comparison with other measurements

So far, there have been only a few reported measurements of PAN in China. The measurement made by Jin and Tian (1982) shows that the concentration of PAN in Lanzhou during 27–28 September 1978 was in the range of 1–17 ppb. Zhang and Tang (1994) reported the first measurements of PAN in Beijing. The observed daily maximum concentrations of PAN during March–June 1990 ranged from 1.1 to 6.8 ppb. Since 2006, measurements of PAN have been made at a few sites in China using modern techniques. The results of these measurements are listed in Table 1. Zhang et al. (2011) made short-term measurements of PAN at Peking University (PKU) and Yufa, Beijing during August 2006 and September 2008, respectively. The reported concentration of PAN at PKU was in the range of 1.21–11.2 ppb, with an average of 1.34 ppb, and that at Yufa was in the range of 0.68–2.51 ppb, with an average of 0.6 ppb. Xu et al. (2011) carried out one week of measurements of PAN at PKU in August 2007 and reported the PAN concentration ranging from 0.31 to 17.81 ppb, with an average of 3.79 ppb. Liu et al. (2010) reported similar high levels of PAN and showed importance of aromatics for the PAN formation in Beijing. The observation of PAN at the Back Gardon site (BGS), Guangzhou, showed an average concentration of 1.32 ppb in July 2006 (Wang et al., 2010). From 23 June to 16 August 2006, Zhang et al. (2009) measured the PAN levels sequentially at a site in Lanzhou City and at the Waliguan (WLG) baseline station,

Qinghai Province. They found that the PAN level at the Lanzhou site ranged from 0.05 to 9.13 ppb, with an average of 0.76 ppb, and that at WLG ranged from 0.08 to 1.41 ppb, with an average of 0.44 ppb. All the above-mentioned measurements were carried out in summer, while our measurements were made in the winter to early spring period. Although our site (CMA) is not far from the PKU site (4.7 km), the observed PAN level was much lower than the summer level at PKU, which may be related to the year-to-year variation but more possibly a result of weaker photochemical production in the cold period. To date, the reported measurements of PAN in Beijing cover only quite short periods of the year. Therefore, the actual seasonal pattern of PAN in Beijing is currently unknown. Nevertheless, the increase trend of PAN, discussed in previous section, and the difference between the summer PAN level at PKU and the winter PAN level at CMA suggest that the PAN level in the urban area of Beijing is higher in warmer months and lower in colder months. Such feature is consistent with those found in Simcoe, Canada (Corkum et al., 1986) and in Lindau and Munich, Germany (Kourtidis et al., 1993; Rappenglück et al., 1993), but inconsistent with those found in Santiago, Chile (Rubio et al., 2007) and in Rishiri Island, Japan (Tanimoto, 2000).

3.3 Diurnal variation

Figure 3 shows the average diurnal cycles of PAN and O_3 at CMA. The O_3 level remained low during the night, increased from about 07:00 LT, until it reached its maximum around 14:00 LT. Similar diurnal patterns of O_3 were observed in Beijing during winter (Lin et al., 2011) and summer (Xu et al., 2011) and in Lanzhou during summer (Zhang et al., 2009). An O_3 peak in the early afternoon usually indicates the significance of photochemical production of O_3. It is reported that even in the wintertime, photochemistry can be a significant source of surface O_3 at CMA (Lin et al., 2011). However, the winter photochemical process alone seems not to be able to cause a daytime O_3 elevation shown in Fig. 3. The meteorological process may have significantly contributed the diurnal variation of O_3. As a photochemical product, PAN is also expected to reach its peak level in the afternoon. Figure 3 shows a PAN peak around

17:00 LT, much later than those found at PKU in summer (Xu et al., 2011; Zhang et al., 2011). Such diurnal pattern of PAN with maximum in late afternoon was also observed in the outflow of the Sacramento urban plume (LaFranchi et al., 2009), in Simcoe, Canada during the wintertime (Corkum et al., 1986), in Atlanta, USA (Williams et al., 1993), and in Lindau, Germany (Kourtidis et al., 1993).

A later PAN peak indicates a longer accumulation time for PAN. In areas of high level NO_2 concentration, the formation of PAN could be fast, leading to no net loss even at elevated temperature environment (Finlayson-Pitts and Pitts, 2000; Gaffney et al., 1999). During our observations, the concentration of NO_2 was very high (4.6–80.2 ppb), with an average of 30.2 ppb. This promoted the production and accumulation of PAN in Beijing and surrounding area. However, high NO_2 concentration does not necessarily cause later PAN peak. For example, Rappenglück et al. (2000) found even peaking of PAN earlier than O_3 in suburban of Santiago de Chile though the NO_2 there was quite high, too. They stated that thermal decompostion of PAN plays a cruical role.

3.4 Relationships among species

Both PAN and O_3 are photochemical products and closely related to NO_x. Therefore, certain relationships among these species are expected. Figure 4 displays the scatter plots showing the O_3-PAN, NO_2-PAN, NO-O_3, and NO_2-O_3 relationships, for daytime and nighttime, respectively. The data in Fig. 4a, b indicate that O_3 is not correlated with PAN at all, inconsistent with the reported positive correlation between both oxidants (e.g. Kourtidis et al., 1993; Liu et al., 2010; McFadyen and Cape, 2005; Rappenglück et al., 1993; Tanimoto, 2000; Wang et al., 2010; Xu et al., 2011). Rappenglück et al. (1993) found good positive correlations between the diurnal maxima of PAN and O_3 in Munich, Germany. They could estimate the background levels of PAN and O_3 based on the results of linear regression analysis. In our case, however, the diurnal maximum of PAN is slightly but significantly ($R^2 = 0.14$, $\alpha = 0.01$) anti-correlated with that of O_3 (figure not shown). And some high levels of PAN (> 2 ppb) occurred only under lower O_3 (< 30 ppb) conditions (see Fig. 4a, b). These phenomena suggest that

during our observations, the variations of the O_3 and PAN concentrations were decoupled and dominated not only necessarily by photochemistry but also by some other processes. However, it is worth pointing out that there was a significant positive correlation ($R^2 = 0.40$) between PAN and total oxidant O_x ($O_3 + NO_2$) (Fig. 5). Since O_x is less subject to the influence of dark reaction ($O_3 + NO$), it is a better indicator of photochemistry than O_3. The significant PAN-O_x correlation indicates that photochemistry did play an important role in enhancing the PAN level. Actually, some quite high PAN levels, particularly those over 1.5 ppb, occurred during the daytime when O_3 was in the range of 10–30 ppb.

Although PAN is not coherent with O_3, it presents a positive correlation with NO_2 (Fig. 4c, d), with a correlation coefficient of 0.63 ($R^2 = 0.40$) for daytime and 0.61 ($R^2 = 0.37$) for nighttime. This correlation demonstrates the importance of NO_2 in the formation of PAN and also suggests that NO_2 could be a better indicator of the PAN plume than O_3 in our case. It should be mentioned that our NO_x analyzer uses a molybdenum converter to reduce NO_2 to NO. This type of converter is known to be subject to interferences from HNO_3, PAN, other organic nitrates. At remote or rural sites, HNO_3 and PAN may contribute substantially to the observed NO_2, leading to overestimated NO_2 levels (Steinbacher et al., 2007). However, our measurements were made at a highly polluted urban site, where the observed average concentration of NO_2 (31 ppb) largely exceeded that of PAN (0.70 ppb). The measured NO_2 concentration may contain only negligible contribution from PAN. Therefore, the significant NO_2-PAN correlation cannot be attributable to the interference from PAN rather to chemical cause.

In addition to the O_3-PAN and NO_2-PAN relationships, we are also interested in the relationships between NO/NO_2 and O_3 during our observations. As shown in Fig. 4e–h, there is a nearly hyperbolic relationship between the O_3 and NO concentrations, and NO_2 shows a highly significant (daytime: $R^2 = 0.70$; nighttime: $R^2 = 0.69$) anti-correlation with O_3. The above relationships among species suggest that there are two pollution patterns that are incompatible with each other. The one is characterized by high PAN, NO and NO_2 levels, the other by high O_3 level. Chemical processes are

important in the formation of the two pollution patterns, but meteorological conditions may be even more important, as discussed in the next sections.

3.5 Impacts from wind speed and direction

Many meteorological factors can exert significant impacts on the concentrations of photochemical oxidants and their precursors, as already shown in the literature (e.g. Rappenglück et al., 1993, 2000). For the CMA site in wintertime, wind speed and direction are two key meteorological factors influencing the concentrations of pollutants in the surface layer. A typical example of such meteorological influence can be demonstrated using the O_3 and NO_x data. Usually, NO_x in urban area is mainly composed of NO emitted by vehicles (Gaffney et al., 1997). Under weak photochemical conditions in wintertime, particularly during nights, abundant NO can cause rapid removal of O_3 and increase of NO_2 in the boundary layer. This may lead to relationships shown in Figs. 4e–h. The chemical balance can be disturbed by stronger winds. Figure 6 shows the influences of wind speed on the NO and O_3 concentrations and on the difference between NO and O_3 concentrations. Under lower wind speeds, the concentrations of NO and O_3 seem to be independent of wind speed. Under higher wind speeds ($> 3\,m\,s^{-1}$), however, the NO concentration is suppressed and the O_3 concentration shows a positive correlation with wind speed ($R^2 = 0.42$, $\alpha = 0.01$). Such influences of wind speed on the NO and O_3 concentrations lead to a logarithmic dependence of ([NO] – [O_3]) on wind speed (Fig. 6c). Under higher wind speeds (say, $> 3\,m\,s^{-1}$), ([NO] – [O_3]) is negatively correlated with wind speed (logarithmic curve distribution), and otherwise, it is independent of wind speed.

In the urban boundary layer O_3 originates partly from local photochemical production and partly from transport. However, the photochemical source of O_3 in winter is quite weak even in the polluted urban area in Beijing. The average photochemical source of surface O_3 in the winter 2007–2008 in Beijing was about $5\,ppb\,day^{-1}$, according to the estimate of Lin et al. (2011). This is a very small source in comparison with the

chemical sink due to NO titration under high levels of NO, not to mention the other sinks. There must be a larger source other than photochemistry for sustaining the O_3 level observed in the surface layer. Transport or mixing of O_3-richer air from the upwind areas and higher altitudes are the additional source of surface O_3. Such transport is promoted by dynamic and thermodynamic processes, such as strong wind, the daytime enhancement of mixing layer height, etc. Our results in Fig. 6 imply that wind speed higher than $3\,m\,s^{-1}$ or a net photochemical production of O_3 is necessary to sustain a certain level of O_3, otherwise, surface O_3 may be fully consumed by NO.

The surface concentrations of pollutants are influenced not only by wind speed but also by wind direction. Figure 7 shows wind roses of wind speed, O_3, PAN, NO_2, NO and CO mixing ratios for the measurement period. As can be seen in Fig. 7a, stronger winds are mainly from the WNW-N sector, reflecting the most remarkable feature of winter monsoon in North China. The observed pollutant concentrations depend very much on wind direction. The rose pattern of O_3 (Fig. 7b) looks similar to that of wind speed, with higher levels under WNW-N winds. The concentrations of PAN, NO_2 and CO show similar dependence on wind direction, with higher values under NNE-W winds and very low values under WNW wind. The pattern of NO looks similar to that of CO, but the NO concentrations under SSE-W winds are relatively low, probably due to more titration of O_3.

In North China, emission sources of gaseous pollutants are mainly distributed in the NE-SE-WS sector relative to Beijing (Zhao et al., 2012). In addition, our site is located in the northwest quadrant of Beijing urban area (see Fig. 1 and Lin et al., 2011). These factors can partly explain the rose patterns of primary pollutants. Another important factor is the change of wind speed with the direction. Stronger WNW-N winds promote the O_3 level and lower the levels of the primary pollutants as well as PAN, while weaker winds from other directions cause transport of primary pollutants to and accumulate over the observation site, and higher NO concentrations under these conditions remove more O_3.

In Fig. 7, we can see again a decoupling between the O_3 and PAN concentrations. Such decoupling feature is demonstrated in detail in Fig. 8, in which the concentration levels of PAN and O_3 are associated with wind speed and direction. It is clear that O_3 and PAN react totally oppositely upon the changes of wind speed and direction. Under stronger winds ($> 4\,m\,s^{-1}$, mainly WSW-NNE), the concentration of PAN stay low (< 1 ppb), while that of O_3 is high (> 20 ppb). Under weaker winds ($< 4\,m\,s^{-1}$), however, most of the observed concentrations of PAN are higher than 0.5 ppb, while those of O_3 are lower than 20 ppb. Since photochemistry makes both O_3 and PAN, the opposite behavior of both oxidants must have been caused by processes other than photochemistry. We believe that, one of the processes is dark reaction between O_3 and NO, which can effectively remove O_3 but has less direct influence on PAN, the other is transport of background air containing higher O_3 and lower PAN, which enhance the level of surface O_3 but not that of PAN.

To further demonstrate impacts of transport, we calculated backward trajectories of air masses arriving at our site during the observations. Totally 660 trajectories (24-h back; every 2 h) were calculated for 55 intact observation days and they were grouped into three clusters. Figure 9 shows the clusters of trajectories and the statistics of pollutants associated with different clusters of trajectories. Cluster 1 represents trajectories that moved highest and fastest from the WNW-NW sector. Cluster 2 represents trajectories that originated from the W-N sector but moved lower and slower than those in cluster 1. Trajectories in cluster 3 originated mainly from the N-E-SW sector and moved lowest and slowest. For most of the time, the mean travelling heights for clusters 1 and 2 are above 1200 and 700 m, respectively. However, the mean travelling height for clusters 3 is lower than 200 m. The mixing layer height observed in urban area of Beijing is normally less than 1200 m, with an average of about 740 m during winter and spring (Cheng et al., 1997). Therefore, air masses in the W-N sector may be transported from the free troposphere, along the trajectories in clusters 1 and 2, downwards to the surface layer.

Normally, O_3 in the nocturnal boundary layer can be removed by dark reactions and dry deposition and O_3 accumulated during the daytime can be stored longer in the residual layer aloft, leading to a positive vertical profile of O_3 in the lower atmosphere (Rappenglück et al., 1993, 2000; Suppan et al., 1998). In our case, i.e. weak photochemistry combined with strong removal of O_3 due to the titration reaction with NO, the level of O_3 in the urban boundary layer may be lower than the background level of O_3 in the winter troposphere, even during the daytime. On the other hand, the primary pollutants, such as CO, NO_x, etc., are emitted and dispersed mainly in the boundary layer. Therefore, the vertical profiles of these species may possess negative gradients. Since PAN shows good correlations with the primary species (see Fig. 7), a negative gradient is also expected. This view of vertical profiles is supported by our data. As can be seen in Fig. 9b, the average O_3 concentrations associated with clusters 1 and 2 are all higher than that with cluster 3 by about a factor of one, while the concentrations of other pollutants (PAN, NO_2, and CO) show a contrary feature, with highest concentrations being associated with cluster 3. As a result, the average PAN/O_3 ratio is found to be 0.023 and 0.031 for air masses associated with clusters 1 and 2, respectively, and 0.11 for air masses associated with cluster 3. These PAN/O_3 ratios are within the range of the ratios reported for different sites and seasons (e.g. Rappenglück et al., 1993; Xu et al., 2011; Zhang et al., 2009, 2011). However, the large differences between the average PAN/O_3 ratios for the boundary layer and the lower free troposphere over a same region are remarkable. We believe that such large differences are mainly caused by strong consumption of O_3 in the boundary layer. The average PAN/CO ratios (ppb/ppb) for the clusters 1, 2, and 3 are 4.7×10^{-4}, 5.4×10^{-4}, and 6.0×10^{-4}, respectively, showing minor differences. However, the average O_3/CO ratios (ppb/ppb) for the clusters 1, 2, and 3 are about 20, 18, and 5, respectively, showing substaintial differences between the boundary layer and the free troposphere. Obviously, there was an O_3 deficiency in the urban boundary layer.

It may be dificult to understand that O_3 is consumed in the boundary layer, while PAN is photochemically produced and accumulated there. To make it clear, lifetimes of PAN

and O_3 were estimated using the observed values of NO, NO_2, and temperature, and rate constants from Atkinson et al. (1997), according to Ridley et al. (1990). Figure 10 shows the time series of estimated PAN and O_3 lifetimes. During the observation period, the lifetime of surface O_3 was mostly less than one hour and never longer than a few hours. In contrast, the lifetime of PAN was mostly in the range of 10–100 h and sometimes even longer than 100 h. The extremely short lifetime of O_3 suppressed the O_3 concentration though there was a weak production of O_3 during the daytime, while the much longer lifetime of PAN favored the accumulation of PAN in the boundary layer.

On the basis of above analyses, we can conclude that higher O_3 level is mainly caused by descending free-tropospheric air from the W-N sector and higher PAN level is due to photochemical formation, transport, and accumulation in the heavily polluted boundary layer. Both chemical and meteorological processes are important causes for the observed decoupling between PAN and O_3.

3.6 A case of mesoscale transport of PAN

Besides local formation and accumulation, PAN in the urban boundary layer of Beijing may be impacted by mesoscale transport. In this section, we discuss a high PAN case, in which mesoscale transport played an important role. Figure 11 displays the time series of PAN, O_3, NO_2 and several meteorological parameters observed during 21–22 February, 2010. During the daytime of 21 February, when relatively strong NW-NE winds blew, the O_3 level was relatively high with a maximum of 41 ppb, but the PAN level stayed quite low. By about 17:00 LT, the NO_2 level started to climb mainly because of the evening rush-hour. Substantial increase of PAN started at about 20:00 LT when the wind changed from NW to SE and became much weaker. After that, the PAN level stayed high till next day. Since PAN is photochemically formed in the atmosphere, the observed nighttime enhancement of the PAN level should be a result of transport of PAN-richer air. The moderate wind speed (about 2–3 $m\,s^{-1}$) and the cold temperature maintained the high PAN level.

To understand the transport process for this case, we produced the corresponding airflow fields in Beijing and surrounding areas using the MICAPS system (http://www.cma.gov.cn/en/Special/2012Special/20120504/index.html). In addition, we simulated the evolution of the wind vector field using the mesoscale model WRF. The real time ground airflow fields at 20:00 and 23:00 LT of 21 February are shown in Fig. 12 and the simulated wind vector fields at four times are shown in Fig. 13.

It can be noticed from Fig. 12 that at 20:00 LT, a convergence zone existed west of Beijing and more rapid airflows only spread over the east of Beijing's urban area. With the movement of the convergence zone towards northwest, the area with rapid airflows approached the observation site. Model results in Fig. 13 match the real time situation fairly well, although the simulated convergence zone was proceeding later in model. The developing of the PAN plume can be well explained using the simulated wind vector fields in Fig. 13. At 15:00 LT, high speed northwest airflow dominated the observation site and large area south of the site. The airflow was weakened by 20:00 LT, and calm wind dominated the site and the area east of it, where PAN and some other pollutants were easily accumulated in the stable condition. Thereafter, the calm wind range was gradually occupied by moderate airflows. By 02:00 LT of 22 February, the site was affected by relatively strong east wind. During the whole process, air over the north part of the North China Plain could be transported to the observation site. And the air transport within the boundary layer was important for our observation, as back trajectories (not shown) indicate that air parcels arriving at the site during the high PAN period travelled only in the lower boundary layer within the last 24 h. Therefore, PAN produced during the daytime within the boundary layer over the E-S sector was transported to our site during the nighttime.

3.7 Estimation of the peroxyacetyl radical (PA) concentration

The PA (CH_3COO_2) radical can play an important role in tropospheric chemistry (Sehested et al., 1998), thus the level and variability of the PA concentration are of interest. Like many other radicals in the atmosphere, direct measurement of the PA radical is

difficult and lacking. Taking advantage of relatively high resolution measurement of PAN and ancillary data of NO_2 and meteorological variables, we can estimate the PA concentration during our observations.

Ambient PAN has no direct emission source and is exclusively formed in the following chemical reaction:

$$CH_3COO_2\,(PA) + NO_2 \rightarrow CH_3COO_2NO_2\,(PAN). \quad (R1)$$

The PA radical is mainly formed in the photochemical oxidation of acetaldehyde, methylvinyl ketone, etc. (LaFranchi et al., 2009; Liu et al., 2010), but it can also be produced in the thermal dissociation of PAN:

$$CH_3COO_2NO_2\,(PAN) \rightarrow CH_3COO_2\,(PA) + NO_2. \quad (R2)$$

One can assume that the Reactions (1) and (2) are balanced (Aneja et al., 1999; Gaffney et al., 1999) so that the equilibrium PA concentration can be estimated as:

$$[PA] = \frac{k_2[PAN]}{k_1[NO_2]} \quad (1)$$

where, k_1 and k_2 are the rate constants for (R1) and (R2), respectively. However, such steady-state treatment may not be appropriate for PAN, which has a lifetime longer than a few hours.

Apart from chemical processes, dynamical and deposition processes can cause the uneven horizontal and vertical distributions of pollutants and influence the variation of PAN as well. In order to accurately describe the variation of PAN at a site, both chemical and physical processes should be taken into account. Theoretically, the rate of change of PAN concentration can be described using:

$$d[PAN]/dt = k_1[PA][NO_2] - k_2[PAN] + phys. \quad (2)$$

For a short time period and under stable atmospheric conditions, the contributions of physical process in (2) can be neglected and formula (2) can be approximated by:

$$d[PAN]/dt = k_1[PA][NO_2] - k_2[PAN]. \quad (3)$$

Since PAN and NO_2 were observed at relatively high resolution, the PA concentration can be estimated as:

$$[PA] = (d[PAN]/dt + k_2[PAN])/k_1[NO_2]. \quad (4)$$

During the observation period, relatively stable atmospheric conditions existed on 7 February, 23 February, and 11 March (no precipitation, wind speed $< 3\,m\,s^{-1}$ all day long). The disturbance from the dynamic processes on these days is considered to be weak compared with the chemical reactions. Therefore, we can estimate the PA levels using Eq. (4). For our calculations, the rate constants k_1 and k_2 are from previous experiments constructed under natural atmospheric conditions and suitable temperature ranges (Atkinson et al., 1997; Demore et al., 1997). Figure 14 shows the estimation results for the three days. As can be seen in this figure, some of the estimated PA concentrations are negative, which is of course unrealistic. We believe that this is mainly caused by the neglect of the physical processes. Diurnal patterns of the estimated PA levels can be obtained by smoothing the high resolution data points, which are subject to dynamical disturbance. Generally, the estimated PA level is higher during daytime and lower during nighttime, consistent with the fact that the PA radical originates mainly from photochemical reactions. The estimated PA levels are in the range of 0–0.01, 0–0.04, and 0–0.04 ppt, with an average of 0.003, 0.006, and 0.005 ppt for 7 February, 23 February, and 11 March, respectively. Based on the measurements from the free troposphere over Washington, USA in August, 1997, Gaffney et al. (1999) estimated the PA concentration to be in the range of 4×10^4–8×10^4 molecules cm^{-3} (0.0015–0.0030 ppt). Using similar method, Aneja et al. (1999) obtained an average PA level of 0.06 ppt (with a maximum 2.17 ppt) for the surface air in Atlanta, Georgia in July and August 1992. Our estimated values of PA concentration are close to those given by

Gaffney et al. (1999) but significantly lower than those reported by Aneja et al. (1999). Seasonal and spatial variations should be the main reason for the differences between the estimated PA levels.

With the above results of PA concentration and other measurements, we have further estimated the contributions to PAN's temporal change from the formation reaction (i.e. $k_1[PA][NO_2]$) and thermal decomposition (i.e. $k_2[PAN]$) of PAN. Temperature and the average NO_2/NO ratio have strong impact on thermal decompositon and hence the lifetime of PAN. The average air temperature ($\pm\sigma$) on 7 February, 23 February, and 11 March was −3.0 (±1.0), 3.2 (±3.1), and 4.9 (±2.6), respectively. The average NO_2/NO ratio ($\pm\sigma$) on 7 February, 23 February, and 11 March was 0.26 (±0.32), 0.43 (±1.14), and 0.13 (±0.11), respectively. The results are displayed in Fig. 15. Just like in Fig. 14, one can see some unrealistic data, which are attributable to dynamical disturbance. The diurnal variations indicate that significant production of PAN occurred mainly during the 09:00–19:00 LT period, particularly around middle to late afternoon. The thermal decomposition of PAN was negligible during the period from midnight to early morning, when colder temperatures dominated. However, it was significant during the other time of the day, particularly around middle to late afternoon, when it was relatively warmer and the PAN level relatively higher. The results shown here suggest that even in the colder months, both photochemical production and thermal decomposition of PAN in the polluted boundary layer over Beijing cannot be neglected, and the former can exceed the later, sustaining a PAN level ranging from 0.23 to 3.51 ppb.

4 Conclusions

Measurements of PAN and some related variables were made at an urban site in Beijing from 25 January to 22 March 2010. The observed PAN concentration ranged from 0.23 to 3.51 ppb, with an average of 0.70 ppb. Although such levels of PAN are much lower than those previously observed during summer at a nearby urban site, they are comparable to the summer PAN levels found at the suburban sites in Beijing,

Guangzhou, and Lanzhou. The average diurnal profile of PAN shows a broad peak around 17:00 LT, while that of O_3 shows a maximum around 14:00 LT. The observed PAN is well correlated with NO_2 but not with O_3. The later peaking phenomenon for PAN and the absence of the O_3-PAN correlation are different from the results of the summer observations in urban Beijing (Liu et al., 2010; Xu et al., 2011) and many other regions.

Our measurements indicate that the variations of the winter concentrations of PAN and O_3 in urban Beijing are decoupled with each other. Further analyses demonstrate that the concentrations of O_3, PAN, and other species were significantly influenced by meteorological processes, particularly, wind conditions and transport of air masses. The winds from the WNW-N sector, which are usually strong during winter in Beijing, can cause higher concentration of surface O_3, but lower concentrations of PAN and the primary pollutants. Under weak winds mainly from the other directions, however, the levels of PAN, NO_x, and CO are significantly enhanced, while that of O_3 decreased. Air masses arriving at our site originate either from the free troposphere over the W-N sector or from the boundary layer over the highly polluted N-S-W sector. The free-tropospheric air shows higher O_3 level and a smaller average PAN/O_3 ratio (< 0.031), while the polluted boundary layer air is abundant in PAN and primary pollutants, with a much larger average PAN/O_3 ratio (0.11). Therefore, the PAN-O_3 decoupling is mainly caused by the air transport conditions and strengthened by rapid removal of surface O_3. Such decoupling, however, does not exclude that PAN and O_3 are simultaneously produced in the boundary layer over urban Beijing and the polluted surrounding regions. In fact, the observed PAN is highly correlated with O_x. This supports the idea that both PAN and O_3 are photochemically formed in the boundary layer, and O_3 formed is rapidly consumed due to the titration reaction $O_3 + NO$, while PAN stays longer under the low temperature condition.

Having the high resolution measurements of PAN and related variables, we were able to estimate the concentration of the PA radical at the urban site in Beijing and calculate the contributions to PAN's change from the formation reaction and thermal

decomposition. For the three selected days with stable atmospheric condition, we obtained daily average PA concentration ranging from 0.003 to 0.006 ppt. We found that PAN was significantly produced during the 09:00–19:00 LT period, particularly around middle to late afternoon, and thermally decomposed from late morning to midnight. Our results suggest that even in the colder period, PAN can be photochemical produced in the boundary layer over Beijing, and the production can exceed the decomposition, sustaining a PAN level from 0.23 to 3.51 ppb. In view of the potential exacerbation of photochemical pollution in and surrounding the megacity Beijing, more observational and modeling studies are needed to characterize the variations of PAN and to assess its impacts on human, vegetation, and the atmospheric chemistry.

Acknowledgements. This work is support by China Special Fund for Meteorological Research in the Public Interest (GYHY201206015, GYHY201106050), Basic Research Fund of CAMS (2011Z003), and National Natural Science Foundation of China (No. 40775074).

References

Aneja, V. P., Hartsell, B. E., Kim, D. S., and Grosjean, D.: Peroxyacetyl nitrate in Atlanta, Georgia: comparison and analysis of ambient data for suburban and downtown locations, J. Air Waste Manage., 49, 177–184, 1999.

Atkinson, R., Baulch, D. L., Cox, R. A., Hampson, R. F., Kerr, J. A., Rossi, M. J., and Tore, J.: Evaluated kinetic, photochemical and heterogeneous data for atmospheric chemistry: supplement V.? IUPAC Subcommittee on Gas Kinetic Data Evaluation for Atmospheric Chemistry, J. Phys. Chem. Ref. Data, 26, 521–1011, 1997.

Beine, H. J. and Krognes, T.: The seasonal cycle of peroxyacetyl nitrate (PAN) in the European Arctic, Atmos. Environ., 34, 933–940, 2000.

Bottenheim, J. W., Gallant, A. G., and Brice, K. A.: Measurements of NO_y species and O_3 at 82° N latitude, Geophys. Res. Lett., 13, 113–116, 1986.

Bottenheim, J. W., Barrie, L. A., and Atlas, E.: The partitioning of nitrogen-oxides in the lower Arctic troposphere during spring 1998, J. Atmos. Chem., 17, 15–27, 1993.

Bottenheim, J. W., Sirois, A., Brice, K. A., and Gallant, A. J.: Five years of continuous observations of PAN and ozone at a rural location in eastern Canada, J. Geophys. Res., 99, 5333–5352, 1994.
Chameides, W. and Walker, J. C. G.: A photochemical theory of tropospheric ozone, J. Geophys. Res., 78, 8751–8760, 1973.
Cheng, S., Xi, D., Zhang, B., Hao, R., Zheng, Z., and Han, T.: Study on the determination and calculating method of atmospheric mixing layer height, China Environmental Science, 17, 512–516, 1997.
Corkum, R., Giesbrecht, W. W., Bardsley, T., and Cherniak, E. A.: Peroxyacetyl nitrate (PAN) in the atmosphere at Simcoe, Canada, Atmos. Environ., 20, 1241–1248, 1986.
Cox, R. A. and Roffey, M. J.: Thermal decomposition of peroxyacetylnitrate in the presence of nitric oxide, Environ. Sci. Technol., 11, 900–906, 1977.
Crutzen, P. J.: The role of NO and NO_2 in the chemistry of the troposphere and stratosphere, Annu. Rev. Earth Pl. Sc., 7, 443–472, 1979.
Dassau, T. M., Shepson, P. B., Bottenheim, J. W., and Ford, K. M.: Peroxyacetyl nitrate photochemistry and interactions with the Arctic surface, J. Geophys. Res., 109, 18302–18316, 2004.
Demore, W. B., Sander, S. P., Golden, D. M., Hampson, R. F., Kurylo, M. J., Howard, C. J., Ravishankara, A. R., Kolb, C. E., and Molina M. J.: Chemical kinetics and photochemical data for use in stratospheric modeling, JPL Publication, 97-4, 1–266, 1997.
Derwent, R. G. and Jenkin, M. E.: Hydrocarbons and the long-range transport of ozone and pan across Europe, Atmos. Environ., 25, 1661–1678, 1991.
Ding, A. J., Wang, T., Thouret, V., Cammas, J.-P., and Nédélec, P.: Tropospheric ozone climatology over Beijing: analysis of aircraft data from the MOZAIC program, Atmos. Chem. Phys., 8, 1–13, doi:10.5194/acp-8-1-2008, 2008.
Draxler, R. R. and Hess, G. D.: Description of the HYSPLIT_4 Modeling System, NOAA Tech. Memo. ERL ARL-224, NOAA Air Resources Laboratory, Silver Spring, MD, 24 pp., 1997.
Ferrier, B. S., Lin, Y., Black, T., Rogers, E., and DiMego, G.: Implementation of a new grid-scale cloud and precipitation scheme in the NCEP Eta model, in: Proceedings of the 15th Conference on Numerical Weather Prediction, American Meteorological Society, San Antonio, Tex, USA, 280–283, 2002.

Finlayson-Pitts, B. J. and Pitts, J. N.: Upper and Lower atmosphere, Academic Press, San Diego, California, 2000.
Fischer, E. V., Jaffe, D. A., and Weatherhead, E. C.: Free tropospheric peroxyacetyl nitrate (PAN) and ozone at Mount Bachelor: potential causes of variability and timescale for trend detection, Atmos. Chem. Phys., 11, 5641–5654, doi:10.5194/acp-11-5641-2011, 2011.
Gaffney, J. S., Marley, N. A., and Prestbo, E. W.: Peroxyacyl nitrates (PANS): their physical and chemical properties, in: Handbook of Environmental Chemistry, Volume 4/Part B, edited by: Hutzinger, O., Springer-Verlag, Berlin, Germany, 1989.
Gaffney, J. S., Marley, N. A., and Prestbo, E. W.: Measurements of peroxyacetyl nitrate at a remote site in the southwestern United States: tropospheric implications, Environ. Sci. Technol., 27, 1905–1910, 1993.
Gaffney, J. S., Marley, N. A., Martin, R. S., Dixon, R. W., Reyes, L. G., and Popp, C. J.: Potential air quality effects of using ethanol-gasoline fuel blends: a field study in Albuquerque, New Mexico, Environ. Sci. Technol., 31, 3053–3061, 1997.
Gaffney, J., Marley, N., Steele, H. D., Drayton, P. J., and Hubbe, J. M.: Aircraft Measurements of nitrogen dioxide and peroxyacyl nitrates using luminol chemiluminescence with fast capillary gas chromatography, Environ. Sci. Technol., 33, 3285–3289, 1999.
Grosjean, D.: Aldehydes, carboxylic acids and inorganic nitrate during NSMCS, Atmos. Environ., 22, 1637–1648, 1988.
Grosjean, D.: Ambient PAN and PPN in southern California from 1960 to the SCOS97-NARSTO, Atmos. Environ., 37, S221–S238, 2003.
Grosjean, E., Grosjean, D., Woodhouse, L. F., and Yang, Y.-J.: Peroxyacetyl nitrate and peroxypropionyl nitrate in Porto Alegre, Brazil, Atmos. Environ., 36, 2405–2419, 2002.
Hong, S.-Y. and Dudhia, J.: Testing of a new non-local boundary layer vertical diffusion scheme in numerical weather prediction applications, 20th Conference on Weather Analysis and Forecasting/16th Conference on Numerical Weather Prediction, Seattle, WA, 2003.
Hudman, R. C., Jacob, D. J., Cooper, O. R., Evans, M. J., Heald, C. L., Park, R. J., Fehsenfeld, F., Flocke, F., Holloway, J., Hübler, G., Kita, K., Koike, M., Kondo, Y., Neuman, A., Nowak, J., Oltmans, S., Parrish, D., Roberts, J. M., and Ryerson, T.: Ozone production in transpacific Asian pollution plumes and implications for ozone air quality in California, J. Geophys. Res., 109, 1–14, 2004.
Jacobi, H.-W., Weller, R., Bluszcz, T., and Schrems, O.: Latitudinal distribution of peroxyacetyl nitrate (PAN) over the Atlantic Ocean, J. Geophys. Res., 104, 26901–26912, 1999.

Jacobi, H.-W., Weller, R., Jones, A. E., Anderson, P. S., and Schrems, O.: Peroxyacetyl nitrate (PAN) concentrations in the Antarctic troposphere measured during the photochemical experiment at Neumayer (PEAN'99), Atmos. Environ., 34, 5235–5247, 2000.

Jin, S. and Tian, Y.: A chromatographic analysis of ambient peroxyacetyl nitrate (PAN), Environm. Sci., 3, 45–47, 1982.

Kleindienst, T. E., Shepson, P. B., Smith, D. F., Hudgens, E. E., Nero, C. M., Cupitt, L. T., Bufalini, J. J., Claxton, L. D., and Nestman, F. R.: Comparison of mutagenic activities of several peroxyacyl nitrates, Environ. Mol. Mutagen., 16, 70–80, 1990.

Kourtidis, K. A., Fabian, P., Zerefos, C., and Rappenglück, B.: Peroxyacetyl nitrate (PAN), peroxypropionyl nitrate (PPN) and PAN/ozone ratio measurements at three sites in Germany, Tellus B, 45, 442–457, 1993.

LaFranchi, B. W., Wolfe, G. M., Thornton, J. A., Harrold, S. A., Browne, E. C., Min, K. E., Wooldridge, P. J., Gilman, J. B., Kuster, W. C., Goldan, P. D., de Gouw, J. A., McKay, M., Goldstein, A. H., Ren, X., Mao, J., and Cohen, R. C.: Closing the peroxy acetyl nitrate budget: observations of acyl peroxy nitrates (PAN, PPN, and MPAN) during BEARPEX 2007, Atmos. Chem. Phys., 9, 7623–7641, doi:10.5194/acp-9-7623-2009, 2009.

Lin, W., Xu, X., Zhang, X., and Tang, J.: Contributions of pollutants from North China Plain to surface ozone at the Shangdianzi GAW Station, Atmos. Chem. Phys., 8, 5889–5898, doi:10.5194/acp-8-5889-2008, 2008.

Lin, W., Xu, X., Ge, B., and Liu, X.: Gaseous pollutants in Beijing urban area during the heating period 2007–2008: variability, sources, meteorological, and chemical impacts, Atmos. Chem. Phys., 11, 8157–8170, doi:10.5194/acp-11-8157-2011, 2011.

Liu, Z., Wang, Y., Gu, D., Zhao, C., Huey, L. G., Stickel, R., Liao, J., Shao, M., Zhu, T., Zeng, L., Liu, S.-C., Chang, C.-C., Amoroso, A., and Costabile, F.: Evidence of reactive aromatics as a major source of peroxy acetyl nitrate over China, Environ. Sci. Technol., 44, 7017–7022, 2010.

Marley, N. A., Gaffney, J. S., Ramos-Villegas, R., and Cárdenas González, B.: Comparison of measurements of peroxyacyl nitrates and primary carbonaceous aerosol concentrations in Mexico City determined in 1997 and 2003, Atmos. Chem. Phys., 7, 2277–2285, doi:10.5194/acp-7-2277-2007, 2007.

McFadyen, G. G. and Cape, J. N.: Peroxyacetyl nitrate in eastern Scotland, Sci. Total Environ., 337, 213–222, 2005.

Monin, A. S. and Obukhov, A. M.: Basic laws of turbulent mixing in the surface layer of the atmosphere, Tr. Akad. Nauk SSSR Geophiz. Inst, 24, 163–187, 1954.

Nielsen, T., Samuelsson, U., Grennfelt, P., and Thomsen, E. L.: Peroxyacetyl nitrate in long-range transported polluted air, Nature, 293, 553–555, 1981.

Peak, M. J. and Belser, W. L.: Some effects of the air pollutant, peroxyacetyl nitrate, upon deoxyribonucleic acid and upon nucleic acid bases, Atmos. Environ., 3, 385–394, 1969.

Rappenglück, B., Kourtidis, K., and Fabian, P.: Measurements of ozone and peroxyacetyl nitrate (PAN) in Munich, Atmos. Environ., 27, 293–305, 1993.

Rappenglück, B., Oyola, P., Olaeta, I., and Fabian, P.: The evolution of photochemical smog in the Metropolitan Area of Santiago de Chile, J. Appl. Meteorol., 39, 275–290, 2000.

Rappenglück, B., Melas, D., and Fabian, P.: Evidence of the impact of urban plumes on remote sites in the Eastern Mediterranean, Atmos. Environ., 37, 1853–1864, 2003.

Rappenglück, B., Forster, C., Jakobi, C., and Pesch, M.: Unusually high levels of PAN and ozone over Berlin, Germany, during nighttime on 7 August, 1998, Atmos. Environ., 38, 6125–6134, 2004.

Roberts, J. M., Flocke, F., Stroud, C. A., Hereid, D., Williams, E., Fehsenfeld, F., Brune, W., Martinez, M., and Harder, H.: Ground-based measurements of peroxycarboxylic nitric anhydrides (PANs) during the 1999 Southern Oxidants Study Nashville Intensive, J. Geophys. Res., 107, 4554, doi:10.1029/2001JD000947, 2002.

Roberts, J. M., Marchewka, M., Bertman, S. B., Sommariva, R., Warneke, C., de Gouw, J., Kuster, W., Goldan, P., Williams, E., Lerner, B. M., Murphy, P., and Fehsenfeld, F. C.: Measurements of PANs during the New England air quality study 2002, J. Geophys. Res., 112, D20306, doi:10.1029/2007JD008667, 2007.

Ridley, B. A., Shetter, J. D., Grandrud, B. W., Salas, L. J., Singh, H. B., Carroll, M. A., Hubler, G., Albritton, D. L., Hastie, D. R., Schiff, H. I., Mackay, G. I., Karecki, D. R., Davis, D. D., Bradshaw, J. D., Rodgers, M. O., Sandholm, S. T., Torres, A. L., Condon, E. P., Gregory, G. L., and Beck, S. M.: Ratios of peroxyacetyl nitrate to active nitrogen observed during aircraft flights over the eastern Pacific Ocean and continental United States, J. Geophys. Res., 95, 10179–10192, 1990.

Rubio, M. A., Gramsch, E., Lissi, E., and Villena, G.: Seasonal dependence of peroxyacetylnitrate (PAN) concentrations in downtown Santiago, Chile, Atmósfera, 20, 319–328, 2007.

Schmitt, R. and Volz-Thomas, A.: Climatology of ozone, PAN, CO, and NMHC in the free troposphere over the Southern North Atlantic, J. Atmos. Chem., 28, 245–262, 1997.

Schrimpf, W., Lienaerts, K., Muller, K. P., Rudolph, J., Neubert, R., Schubler, W., and Levin, I.: Dry deposition of peroxyacetyl nitrate (PAN): Determination of its deposition velocity at night from measurements of the atmospheric PAN and ^{222}Radon concentration gradient, Geophys. Res. Lett., 23, 3599–3602, 1996.

Sehested, J., Christensen, L. K., Møgelberg, O. J., Nielsen, O. J., Wallingon, T. J., Guschin, A., Orlando, J. J., and Tyndall, G. S.: Absolute and relative rate constants for the reactions $CH_3C(O)O_2 + NO$ and $CH_3C(O)O_2 + NO_2$ and Thermal Stability of $CH_3C(O)O_2NO_2$, J. Phys. Chem., 102, 1779–1789, 1998.

Singh, H. B.: Reactive nitrogen in the troposphere, Environ. Sci. Technol., 21, 320–327, 1987.

Singh, H. B. and Salas, L. J.: Methodology for the analysis of peroxyacetyl nitrate (PAN) in the unpolluted atmosphere, Atmos. Environ., 17, 1507–1516, 1983a.

Singh, H. B. and Salas, L. J.: Peroxyacetyl nitrate in the free troposphere, Nature, 302, 326–328, 1983b.

Singh, H. B. and Salas, L. J.: Measurements of peroxyacetyl nitrate (pan) and peroxypropionyl nitrate (ppn) at selected urban, rural and remote sites, Atmos. Environ., 23, 231–238, 1989.

Singh, H. B., Herlth, D., O'Hara, D., Zahnle, K., Bradshaw, J. D., Sandholm, S. T., Talbot, R., Crutzen, P. J., and Kanakidou, M.: Relationship of peroxyacetyl nitrate to active and total odd nitrogen at northern high latitudes: influence of reservoir species on NO_x and O_3, J. Geophys. Res., 97, 16523–16530, 1992.

Skamarock, W. C. and Klemp, J. B.: A time-split nonhydrostatic atmospheric model for weather research and forecasting applications, J. Comput. Phys., 227, 3465–3485, 2008.

Staehelin, J., Harris, N. R. P., Appenzeller, C., and Eberhard, J.: Ozone trends: A review, Rev. Geophys., 39, 231–290, 2001.

Steinbacher, M., Zellweger, C., Schwarzenbach, B., Bugmann, S., Buchmann, B., Ordóñez, C., Prevot, A. S. H., and Hueglin, C.: Nitrogen oxide measurements at rural sites in Switzerland: bias of conventional measurement techniques, J. Geophys. Res., 112, D11307, doi:10.1029/2006JD007971, 2007.

Stephens, E. R.: The formation, reactions and properties of peroxyacyl nitrates in photochemical air pollution, Adv. Environ. Sci., 1, 119–146, 1969.

Stephens, E. R., Hanst, P. L., Doerr, R. C., and Scott, W. E.: Reactions of nitrogen dioxide and organic compounds in air, Ind. Eng. Chem., 48, 1498–1504, 1956.

Suppan, P., Fabian, P., Vyras, L., and Gryning, S. E.: The behaviour of ozone and peroxyacetyl nitrate concentrations for different wind regimes during the MEDCAPHOT-TRACE campaign in the greater area of Athens, Greece, Atmos. Environ., 32, 2089–2102, 1998.

Talukdar, R. K., Burkholder, J. B., Schmoltner, A.-M., Roberts, J. M., Wilson, R. R., and Ravishankara, A. R.: Investigation of the loss processes for peroxyacetyl nitrate in the atmosphere: UV photolysis and reaction with OH, J. Geophys. Res., 100, 14163–14173, 1995.

Tang, G., Li, X., Wang, Y., Xin, J., and Ren, X.: Surface ozone trend details and interpretations in Beijing, 2001–2006, Atmos. Chem. Phys., 9, 8813–8823, doi:10.5194/acp-9-8813-2009, 2009.

Tang, X., Zhang, Y., and Shao, M.: Atmospheric enviornmental chemistry, High Education Press, Beijing, 2001.

Tanimoto, H.: The seasonal variation of atmospheric peroxyacetyl nitrate (PAN) in east Asia observed by GC/NICI-MS technique, Dissertation, The University of Tokyo, 2000.

Taylor, O. C.: Importance of peroxyacetyl nitrate (PAN) as a phytotoxic air pollutant, J. Air Pollut. Control Assoc., 19, 347–351, 1969.

Tuazon, E. C., Carter, W. P. L., and Atkinson, R.: Thermal decomposition of peroxyacetyl nitrate and reactions of acetyl peroxy radicals with NO and NO_2 over the temperature range 283–313 K, J. Phys. Chem., 95, 2434–2437, 1991.

Turnipseed, A. A., Huey, L. G., Nemitz, E., Stickel, R., Higgs, J., Tanner, D. J., Slusher, D. L., Sparks, J. P., Flocke, F., and Guenther A.: Eddy covariance fluxes of peroxyacetyl nitrates (PANs) and NO_y to a coniferous forest, J. Geophys. Res., 111, 9304–9320, 2006.

Volz-Thomas, A., Xueref, I., and Schmitt, R.: Automatic gas chromatograph and calibration system for ambient measurements of PAN and PPN, Environ. Sci. Poll. Res., 9, 72–76, 2002.

Wang, B., Shao, M., Roberts, J. M., Yang, G., Yang, F., Hua, M., Zeng, L., Zhang, Y., and Zhang, J.: Ground-based on-line measurements of peroxyacetyl nitrate (PAN) and peroxypropionyl nitrate (PPN) in the Pearl River Delta, China, Int. J. Environ. An. Ch., 90, 548–599, 2010.

Wang, T., Ding, A., Gao, J., and Wu, W. S.: Strong ozone production in urban plumes from Beijing, China, Geophys. Res. Lett., 33, 21806–21810, 2006.

Wang, Y., Konopka, P., Liu, Y., Chen, H., Müller, R., Plöger, F., Riese, M., Cai, Z., and Lü, D.: Tropospheric ozone trend over Beijing from 2002–2010: ozonesonde measurements and

modeling analysis, Atmos. Chem. Phys., 12, 8389–8399, doi:10.5194/acp-12-8389-2012, 2012.

Whalley, L. K., Lewis, A. C., McQuaid, J. B., Purvis, R. M., Lee, J. D., Stemmler, K., Zellweger, C., and Ridgeon, P.: Two high-speed, portable GC systems designed for the measurement of non-methane hydrocarbons and PAN: results from the Jungfraujoch High Altitude Observatory, J. Environ. Monitor., 6, 234–241, 2004.

Williams, E. L., Grosjean, E., and Grosjean, D.: Ambient levels of the peroxyacetyl nitrates PAN, PPN and MPAN in Atlanta, Georgia, J. Air Waste Manage., 43, 873–879, 1993.

Williams, J., Roberts, J. M., Fehsenfeld, F. C., Bertman, S. B., Buhr, M. P., Goldan, P. D., Hübler, G., Kuster, W. C., Ryerson, T. B., Trainer, M., and Young, V.: Regional ozone from biogenic hydrocarbons deduced from airborne measurements of PAN, PPN, and MPAN, Geophys. Res. Lett., 24, 1099–1102, 1997.

Wu, Y., Wang, R., Zhou, Y., Lin, B., Fu, L., He, K., and Hao, J.: On-road vehicle emission control in Beijing: past, present, and future, Environ. Sci. Technol., 45, 147–153, 2011.

Wu, Z., Wang, X., Turnipseed, A. A., Chen, F., Zhang, L., Guenther, A. B., Karl, T., Huey, L. G., Niyogi, D., Xia, B., and Alapaty, K.: Evaluation and improvements of two community models in simulating dry deposition velocities for peroxyacetyl nitrate (PAN) over a coniferous forest, J. Geophys. Res., 117, 4310–4321, 2012.

Xu, Z., Zhang, J., Yang, G., and Hu, M.: Acyl peroxy nitrate measurements during the photochemical smog season in Beijing, China, Atmos. Chem. Phys. Discuss., 11, 10265–10303, doi:10.5194/acpd-11-10265-2011, 2011.

Zellweger, C., Ammann, M., Buchmann, B., Hofer, P., Lugauer, M., Rüttimann, R., Streit, N., Weingartner, E., and Baltensperger, U.: Summertime NO_y speciation at the Jungfraujoch, 3580 m a.s.l., Switzerland, J. Geophys. Res., 105, 6655–6667, 2000.

Zhang, J. and Tang, X.: Atmospheric PAN measurements and the formation of PAN in various systems, Environ. Chem., 13, 30–39, 1994.

Zhang, J. B., Xu, Z., Yang, G., and Wang, B.: Peroxyacetyl nitrate (PAN) and peroxypropionyl nitrate (PPN) in urban and suburban atmospheres of Beijing, China, Atmos. Chem. Phys. Discuss., 11, 8173–8206, doi:10.5194/acpd-11-8173-2011, 2011.

Zhang, J. M., Wang, T., Ding, A. J., Zhou, X. H., Xue, L. K., Poon, C. N., Wu, W. S., Gao, J., Zuo, H. C., Chen, J. M., Zhang, X. C., and Fan, S. J.: Continuous measurement of peroxyacetyl nitrate (PAN) in suburban and remote areas of western China, Atmos. Environ., 43, 228–237, 2009.

Zhao, B., Wang, P., Ma, J. Z., Zhu, S., Pozzer, A., and Li, W.: A high-resolution emission inventory of primary pollutants for the Huabei region, China, Atmos. Chem. Phys., 12, 481–501, doi:10.5194/acp-12-481-2012, 2012.

Table 1. Statistics of the PAN concentrations observed at a few sites in China (Unit: ppb).

Site	Period	Average	Median	Range	Reference
CMA, Beijing	26 Jan–22 Mar 2010	0.70	0.55	0.23–3.51	This work
PKU, Beijing	15–27 Aug 2006	1.34	0.91	1.21–11.2	Zhang et al. (2011)
Yufa, Beijing	3–12 Sep 2006	0.6	0.15	0.68–2.51	Zhang et al. (2011)
PKU, Beijing	14–19 Aug 2007	3.79	2.53	0.31–17.81	Xu et al. (2011)
BGS,Guangzhou	7–31 Jul 2006	1.32	n.a.	0–4	Wang et al. (2010)
Lanzhou	23 Jun–17 Jul 2006	0.76	n.a.	0.05–9.13	Zhang et al. (2009)
WLG, Qinghai	22 Jul–16 Aug 2006	0.44	n.a.	0.08–1.41	Zhang et al. (2009)

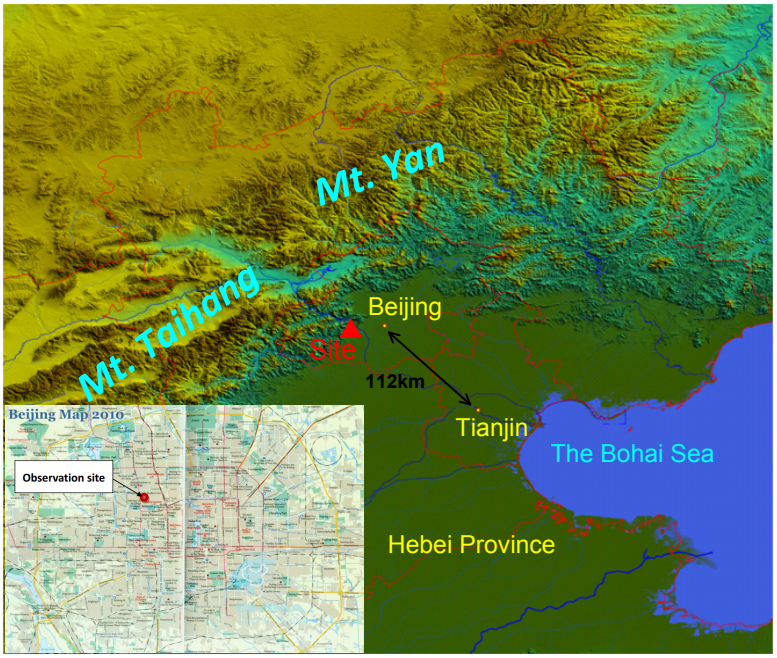

Fig. 1. Map showing the north part of the North China Plain and Beijing city, with the measurement site labeled.

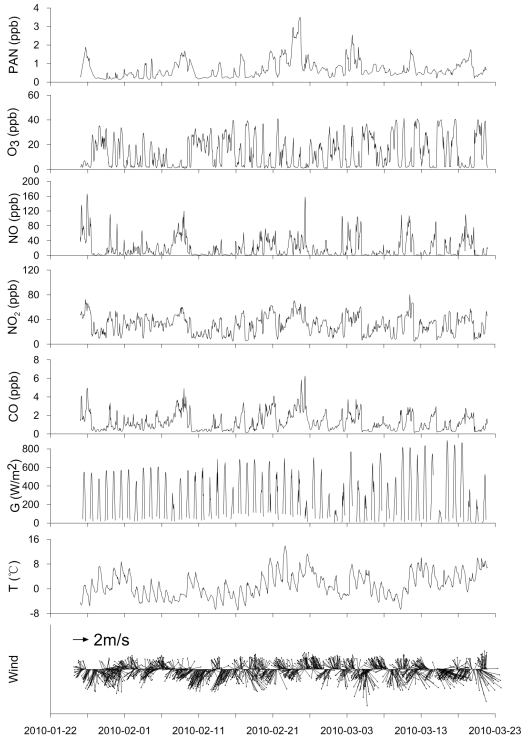

Fig. 2. The time series of hourly mean PAN concentration the PAN, O_3, NO, NO_2, and CO concentrations, together with global radiation (G), temperature (T), and wind vector. Since no measurement of solar radiation available from the CMA site, global radiation from the Shangdianzi (a rural site in Beijing) is plotted.

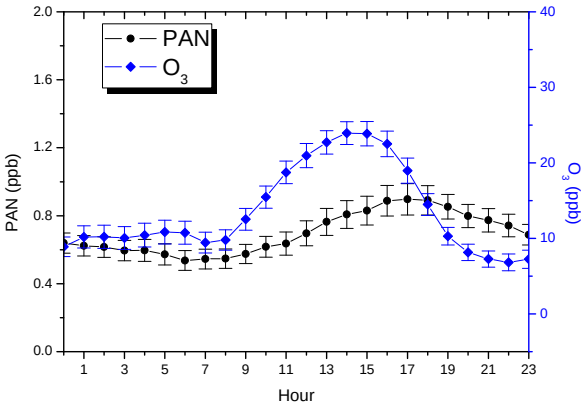

Fig. 3. Diurnal cycles of PAN and O_3 at the CMA site during the wintertime. The vertical bars represent one standard error of the mean.

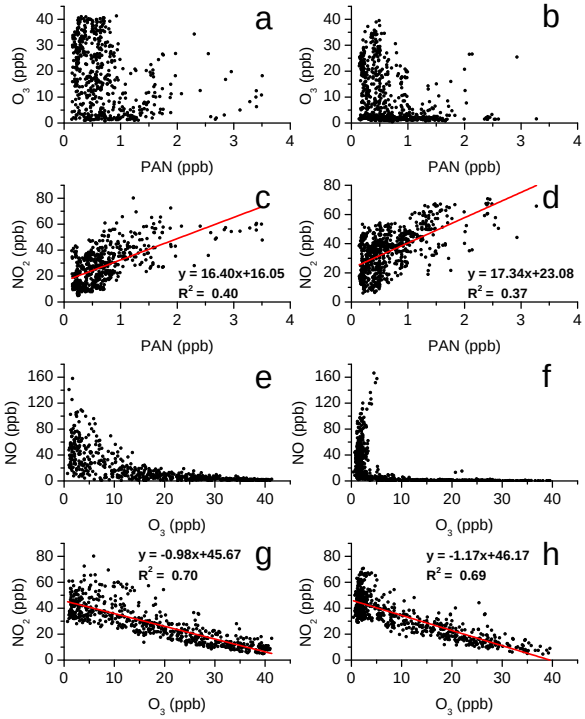

Fig. 4. Scatter plots of hourly averaged O_3 vs. PAN **(a, b)**, NO_2 vs. PAN **(c, d)**, NO vs. O_3 **(e, f)**, and NO_2 vs. O_3 **(g, h)** at the CMA site during the wintertime. Plots on the left side are daytime data and those on the right side are nighttime data. The correlations shown in **(c)**, **(d)**, **(g)**, and **(h)** are significant at $\alpha = 0.01$.

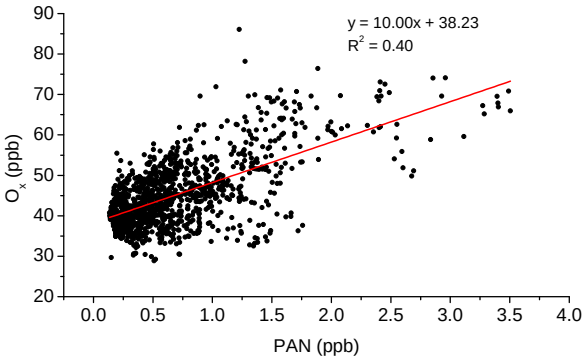

Fig. 5. Correlation between PAN and the total oxidant O_x ($O_3 + NO_2$) in winter Beijing.

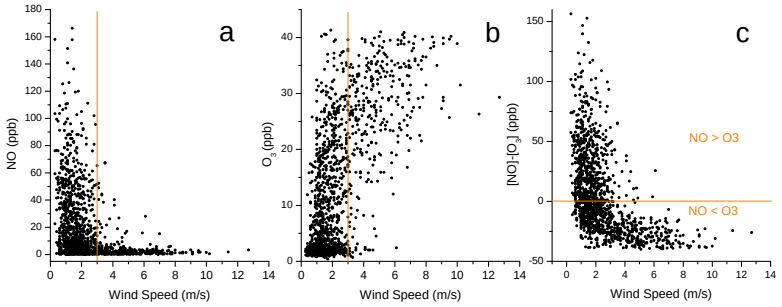

Fig. 6. Influences of wind speed on the concentrations of NO **(a)**, O_3 **(b)** and the difference between NO and O_3 concentrations **(c)** in winter Beijing.

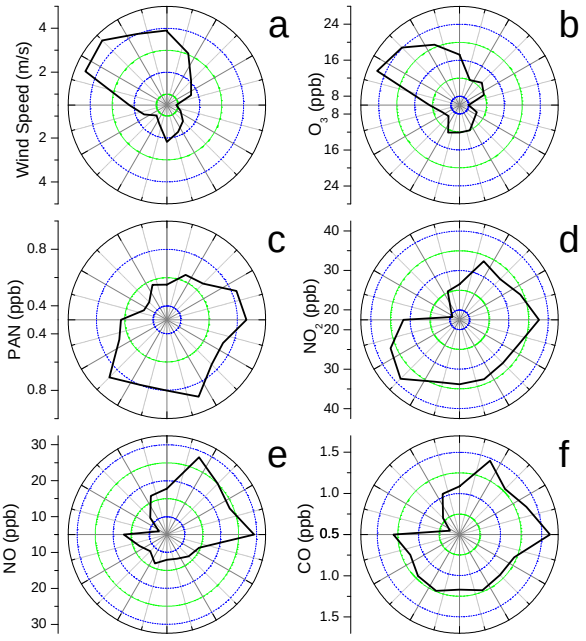

Fig. 7. Wind roses of wind speed **(a)**, O_3 **(b)**, PAN **(c)**, NO_2 **(d)**, NO **(e)**, and CO **(f)** in winter Beijing.

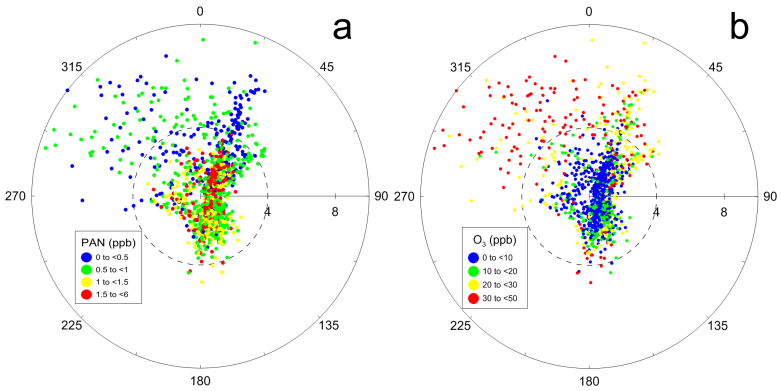

Fig. 8. Scatter plots for the PAN **(a)** and O_3 **(b)** levels observed under different wind directions and speeds.

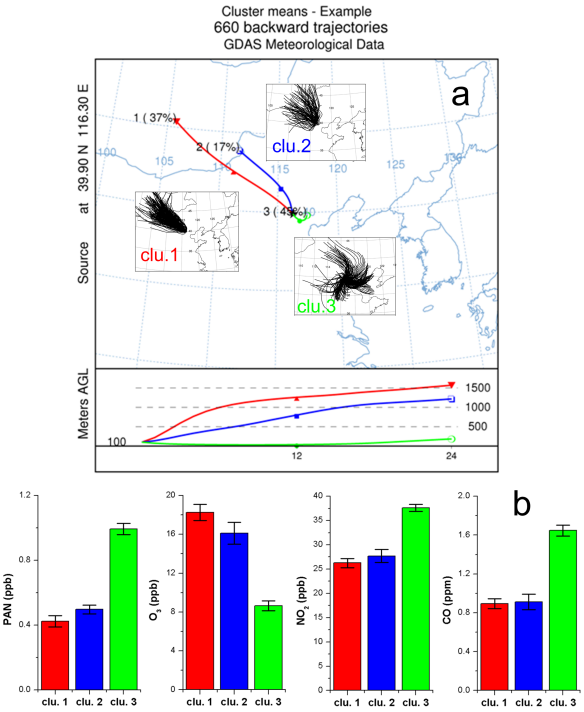

Fig. 9. Back trajectories for airmasses arriving at 100 m above the CMA site during the observation period (every 2 h begining at 00:00 LT, totally 660) and their mean trajectories resulted from the cluster analysis **(a)** and average pollutant concentrations with standard error of the mean for different clusters **(b)**.

Discussion Paper | Discussion Paper | Discussion Paper | Discussion Paper |

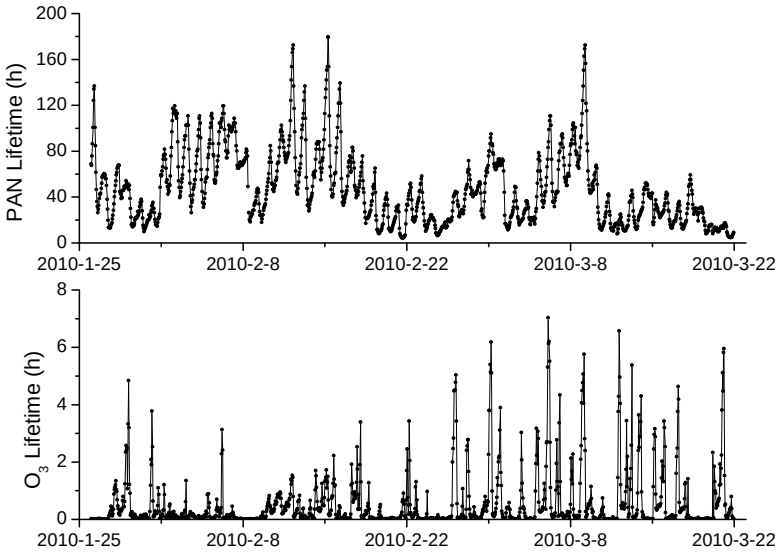

Fig. 10. The estimated lifetimes of PAN and O_3 in the winter boundary layer of Beijing.

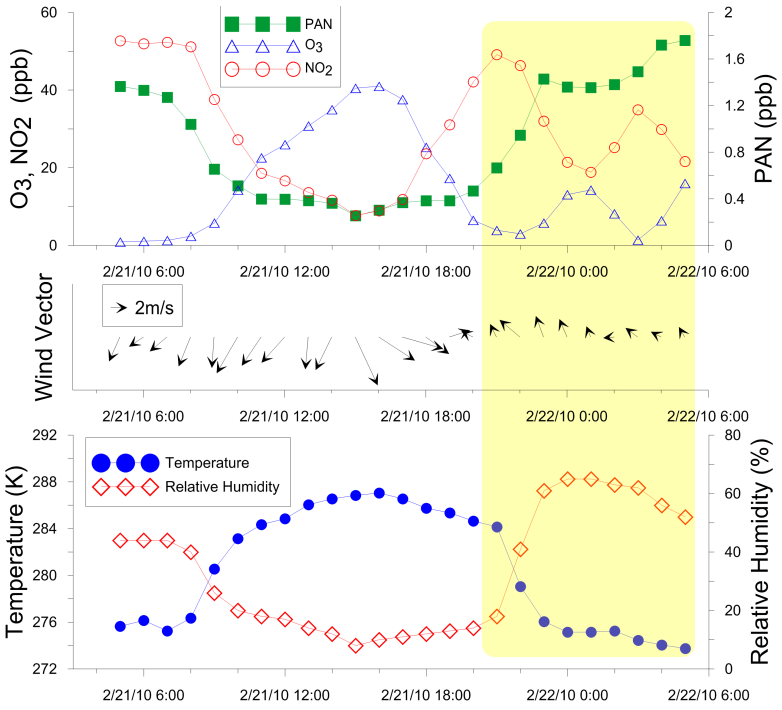

Fig. 11. Time series of **(a)** the pollutant concentrations (PAN, O_3, NO_2) and **(b)** meteorological variables (wind vector, temperature and relative humidity) before and during the transport case.

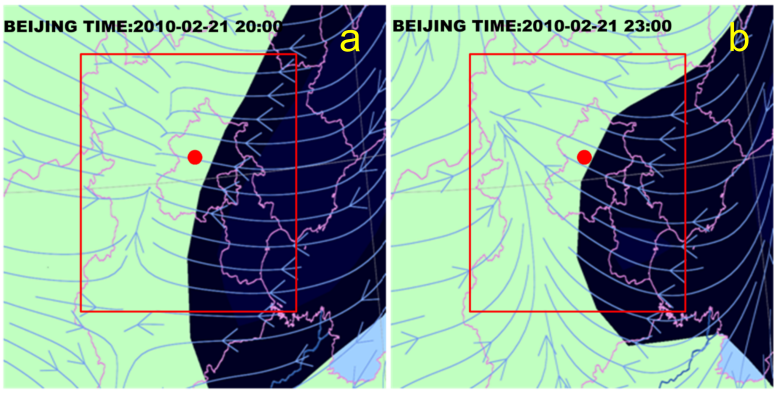

Fig. 12. Real time ground airflow fields at 20:00 LT **(a)** and 23:00 LT **(b)**. Blue lines show the airflow computed by software MICAPS, based on the wind data observed in North China. Regions with wind speed higher than 2 m s^{-1} are shadowed in dark blue. The filled red circles indicate the observation site. The red rectangles indicate the domain for the WRF model simulations (see Fig. 13).

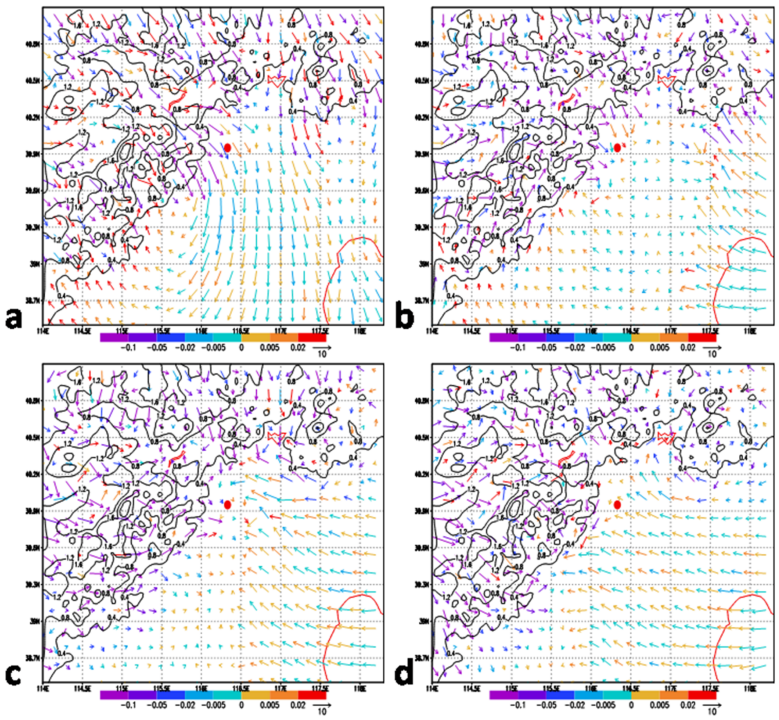

Fig. 13. Simulated wind fields of WRF model for 15:00 LT 21 February **(a)**, 20:00 LT 21 February **(b)**, 23:00 LT 21 February **(c)**, and 02:00 LT 22 February **(d)** in the lower boundary layer. Wind information is presented at the lowest level of sigma vertical coordinate executed in WRF program. Different colors shown with arrows are used to indicate vertical flow speed. The black contour lines reflect the ground altitudes. The filled red circles mark the location of the observation site and the red curves the land border.

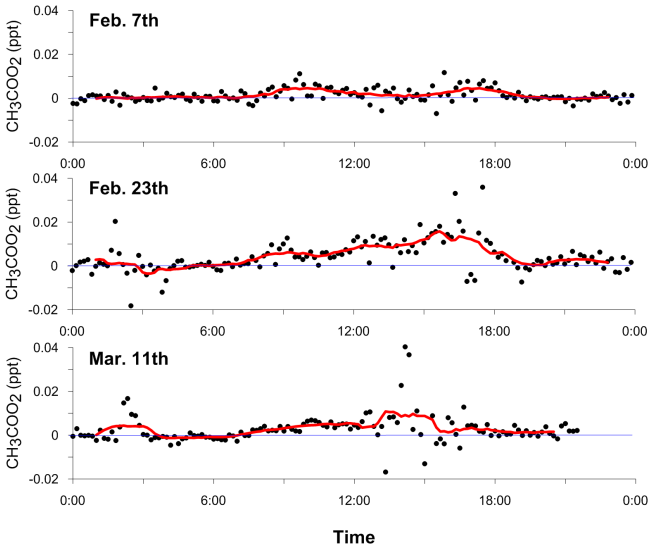

Fig. 14. Estimated concentrations of the CH_3COO_2 (PA) radical at the CMA site on 7 February, 23 February, and 11 March, 2010. The black points are the PA concentrations calculated from 10-min measurements using Eq. (4). The red curves and blue lines represent the moving average (12 points) and the zero value, respectively.

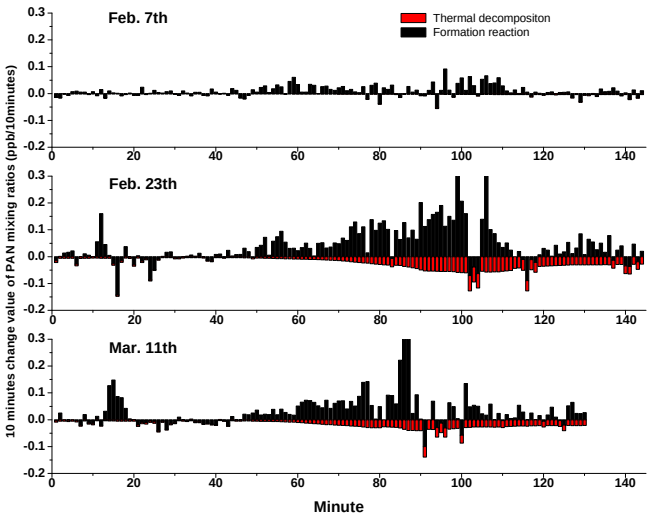

Fig. 15. Calculated contributions to PAN's temporal change from the formation reaction (red) and thermal decomposition (blue) of PAN at the CMA site on 7 February, 23 February, and 11 March 2010. The negative values in the formation contribution are unrealistic and caused by the assumption of no dynamical disturbance to the PAN level.